An Orbital Angular Momentum Mode Estimation Method with an Unknown Beam Axis

1st Gaofeng Shu*†‡ 2nd Bingxu Chen* 3rd Ning Li*†‡
*School of Computer and Information Engineering, Henan University
†Henan Engineering Research Center of Intelligent Technology and Application, Henan University
‡Henan Key Laboratory of Big Data Analysis and Processing, Henan University
Kaifeng 475004, Henan, China
gaofeng.shu@henu.edu.cn chenbingxu@henu.edu.cn hedalining@henu.edu.cn

2021 IEEE Sensors | 978-1-7281-9501-8/21/$31.00 ©2021 IEEE | DOI: 10.1109/SENSORS47087.2021.9639834

***Abstract*—Orbital angular momentum (OAM) beam is very difficult to receive due to the divergence of the beam. The position of the beam axis must be known by the existing receiving methods, including the single point method and the phase gradient method. This article proposes an OAM mode estimation method with an unknown beam axis. This method first estimates the position of the beam axis according to the phase characteristics and then uses the phase gradient method to estimate the OAM mode. The simulation results verify the effectiveness of the method.**

***Index Terms*—Orbital angular momentum (OAM), OAM detection, OAM mode estimation, phase gradient method**

I. Introduction

The application of light beams or electromagnetic (EM) waves carrying orbital angular momentum (OAM), also called vortex beam [1], is rapidly developed during the past few decades [2]–[4]. Vortex beams have a helical phase wavefront of $\exp(\mathrm{j}l\varphi)$ term, where φ is the transverse azimuthal angle around the propagation direction and l is an integer indicating the OAM mode [3], [5].

For radio vortex beam, the helical phase wavefront is introduced by the feed with a linear phase gradient in the azimuthal angle [6]. As a result, there is a phase singularity along the beam axis [7], where its electric field (E-field) is zero, resulting in a "doughnut" intensity profile [8] and a divergent beam [9].

The centrally hollow and divergent characteristics make it very difficult to detect OAM waves in full aperture over a long distance. In 2010, Mohammadi *et al.* [10] introduced the single-point method and the phase gradient method to estimate the OAM modes of radio vortex wave. For the phase gradient method, one should measure the phase difference between two or more points on a circle or a circle segment with the circle center on the beam axis [11]–[13]. Some other methods, such as partial aperture sampling reception (PASR) [14], [15] and variable scale aperture sampling reception (VSASR) [16], are both variants of the phase gradient method. As an emerging method, metasurface reception is a full-aperture reception method, which requires the beam axis to coincide with the receiving antenna center [17]–[19].

This work was supported by the National Natural Science Foundation of China (61871175), and the Plan of Science and Technology of Henan Province (212102210093, 212102210101). (Corresponding author: Ning Li.)

The position of the beam axis must be known when all methods mentioned above are used to estimate the OAM mode. As far as we know, there is currently no such OAM mode estimation method in the published literature when the beam axis is unknown.

In this article, we propose an OAM mode estimation method with an unknown beam axis. In this method, the phase characteristics of the vortex beam on the plane perpendicular to the beam axis are analyzed, and then the position of the beam axis is estimated by the phase characteristics. Finally, the phase gradient method is applied to evaluate the OAM mode.

This article is organized as follows. In Section II, we introduced the basic principles of the proposed method, including the analysis of the phase characteristics of the OAM beams and the steps of the proposed method. In Section III, some simulation results based on the proposed method are presented. Finally, Section IV draws the main conclusions and describes future work.

II. Basic Principles

A. The Phase Characteristic of an OAM Beam

The phase expression of the general OAM beam can be expressed as the following form [4],

$$E(k, r, l) = \exp\left(-\mathrm{j}kr\right) \cdot \exp\left(\mathrm{j}l\varphi\right) \tag{1}$$

where $k = 2\pi/\lambda$ is the wave number, λ is the wavelength, r is the distance between the field point and the source point, l is the OAM mode, $\mathrm{j} = \sqrt{-1}$, and φ is the azimuth angle of the field point with respect to the source point. For convenience, the amplitude of the OAM beam is neglected here. The phase distribution on the plane perpendicular to the beam axis is shown in Fig. 1. The phase of a vortex beam is decomposed into the phase caused by the free space and the phase caused by the source.

1) The phase cause by the free space: Let the beam axis be the origin, a polar coordinate system is established, and let the distance between the source and the phase plane be

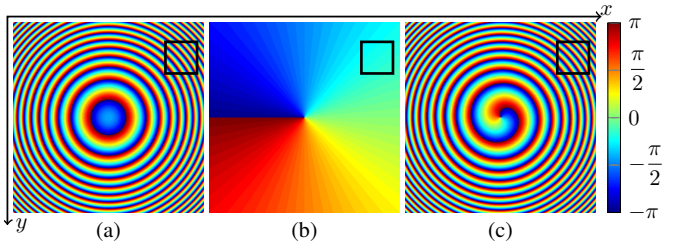

Fig. 1. The components of the phase of a vortex beam. (a) The phase caused by space $\exp(-\mathrm{j}kr)$, (b) the phase only caused by the source of the vortex beam $\exp(\mathrm{j}l\varphi)$, and (c) the addition of these two phases $\exp(-\mathrm{j}kr)\exp(\mathrm{j}l\varphi)$. The black box is a sampling area at the same place.

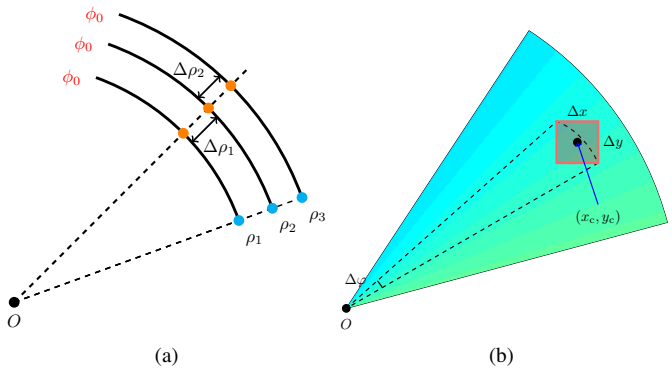

Fig. 2. (a) The isophase lines on the phase plane caused by space with the value of ϕ_0 (solid black lines). The radii of the isophase lines are ρ_1, ρ_2, and ρ_3, respectively. The distances between the adjacent isophase lines are $\Delta\rho_1$ and $\Delta\rho_2$. (b) The sketch figure of E-field reception of a rectangle sampling area, whose center is located at (x_c, y_c), and the dimensions are Δx and Δy. The maximum azimuth angle covered by the sampling area with regard to the origin O is $\Delta\varphi$.

the fixed R_0, so the distance between the point (ρ, φ) on the phase plane and the source is expressed as

$$r = \sqrt{\rho^2 + R_0^2}. \tag{2}$$

It can be seen from (2) that when ρ is constant, r does not change, so the phase $\exp(-\mathrm{j}kr)$ will not change either, as shown in Fig. 1(a). The phase of the E-field is the same on the circles with the same radius and therefore the isophase lines are concentric circles with the beam axis as the center.

Now take any three adjacent isophase lines in Fig. 1(a) for analysis, as shown by the solid black lines in Fig. 2(a). Let the wrapped phase value of the isophase lines be ϕ_0. The radii of the three isophase lines are marked as ρ_1, ρ_2, and ρ_3, respectively. The distances between adjacent isophase lines are noted as $\Delta\rho_1$ and $\Delta\rho_2$. For the general case, $R_0 \gg \rho_1, \rho_2, \rho_3$, so (2) can be simplified to

$$r \approx R_0 + \frac{\rho^2}{2R_0}. \tag{3}$$

Observing Fig. 2(a), we can assume that

$$\phi_0 + 2n\pi = k \cdot \left(R_0 + \frac{\rho_2^2}{2R_0}\right) = kR_0 + \frac{\pi\rho_2^2}{\lambda R_0} \tag{4}$$

where n is an integer. Based on the geometric relationship and the definition of the isophase lines, the phase change caused by the adjacent phase line is 2π, and then

$$\phi_0 + 2n\pi - 2\pi = kR_0 + \frac{\pi\rho_1^2}{\lambda R_0} = kR_0 + \frac{\pi\left(\rho_2 - \Delta\rho_1\right)^2}{\lambda R_0} \tag{5}$$

$$\phi_0 + 2n\pi + 2\pi = kR_0 + \frac{\pi\rho_3^2}{\lambda R_0} = kR_0 + \frac{\pi\left(\rho_2 + \Delta\rho_2\right)^2}{\lambda R_0}. \tag{6}$$

Combining (4)(5)(6), we obtain

$$\rho_2 = \frac{\left(\Delta\rho_1\right)^2 + \left(\Delta\rho_2\right)^2}{2\left(\Delta\rho_1 - \Delta\rho_2\right)}. \tag{7}$$

It can be seen from (7) that for the phase distribution shown in Fig. 1(a), the radii of the three adjacent isophase lines can be calculated by the distance between the adjacent isophase lines, to determine the center of the isophase lines, i.e., the beam axis.

2) The phase caused by the source: The phase caused by the source is only related to the azimuth angle, i.e., the polar angle, as shown in Fig. 1(b). The phase of the E-field is the same along the ray with the same polar angle and therefore the isophase lines are the rays that radiate outward from the beam axis.

Now consider a rectangular sampling area whose center is (x_c, y_c), and the dimensions along the horizontal axis and vertical axis are Δx and Δy, respectively. The sampling area is located in the interval $I = \left[x_c - \frac{\Delta x}{2}, x_c + \frac{\Delta x}{2}\right] \times \left[y_c - \frac{\Delta y}{2}, y_c + \frac{\Delta y}{2}\right]$, as illustrated in the red rectangular box in Fig. 2(b). The azimuth angle covered by the sampling area is denoted by $\Delta\varphi$. If the sampling area is far enough from the beam axis, the azimuth angle covered by the sampling area can be approximated as

$$\Delta\varphi \approx \frac{\sqrt{\left(\Delta x\right)^2 + \left(\Delta y\right)^2}}{\rho_c}. \tag{8}$$

If $\rho_c \gg \sqrt{\left(\Delta x\right)^2 + \left(\Delta y\right)^2}$, the azimuth angle covered by the sampling area is very small, so the phase caused by the source $l\varphi$ can be regarded as a constant.

The true vortex phase is the superposition of the phase caused by space and the phase caused by the feed, as shown in Fig. 1(c), whose isophase lines are helical. It can be seen from Fig. 1(b) that in a small area far from the beam axis, as shown in the black box in Fig. 1, the change of the phase is very small, making the superimposed phase similar to the phase in the same area in Fig. 1(a). Therefore, the isophase lines in this sampling area can be approximated as concentric circles.

B. The Steps of the Proposed Method

According to Section II-A, we propose a method to estimate the transmitting OAM mode. The flow diagram of the

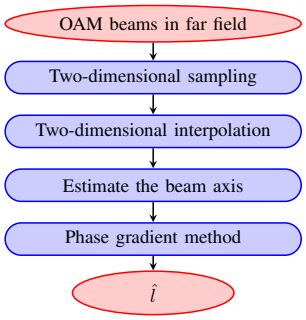

Fig. 3. The flow diagram of the proposed method for OAM estimation.

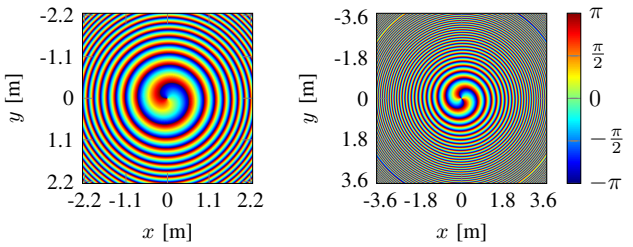

Fig. 4. The phase pattern of the vortex beams with OAM order (a) $l = 1$ or (b)$l = 2$ generated by the same UCA in 4nec2 on the transverse plane in far-field. The plane is 10 m away from the source antenna.

proposed method of OAM mode estimation is illustrated in Fig. 3.

The specific steps are as follows. First, perform two-dimensional rectangular sampling on a plane perpendicular to the beam axis of a vortex beam carrying OAM in the far field. Second, perform two-dimensional interpolation on the E-field value of the samples to make the phase smoother. Third, choose three suitable adjacent isophase lines to determine the coordinates of the beam axis according to (7). Finally, based on the coordinate of the beam axis, the OAM mode is estimated with the help of the phase gradient method.

III. Simulation Results

To verify the effectiveness of the proposed method, this article uses the free software 4nec2 [20] to generate far field OAM beams generated by a uniform annular array (UCA). The UCA is composed of 16 ideal electric dipoles with an array radius of 2λ. The frequency is 9.6 GHz. The phase patterns of OAM mode $l = 1$ and $l = 2$ are shown in Fig. 4.

Based on the flow diagram illustrated in Fig. 3, we first extract the complex E-field of 15×15 sampling points at equal intervals (about 0.07 m) in the area far from the beam axis, as shown in Fig. 5(a). Second, the interpolated E-field is shown in Fig. 5(b), and the arc-shaped isophase lines can be seen. Third, select adjacent isophase lines and draw a perpendicular bisector (blue line in Fig. 5(c)) based on geometric properties. The perpendicular bisector and the three isophase lines intersect at points A, B, and C, respectively.

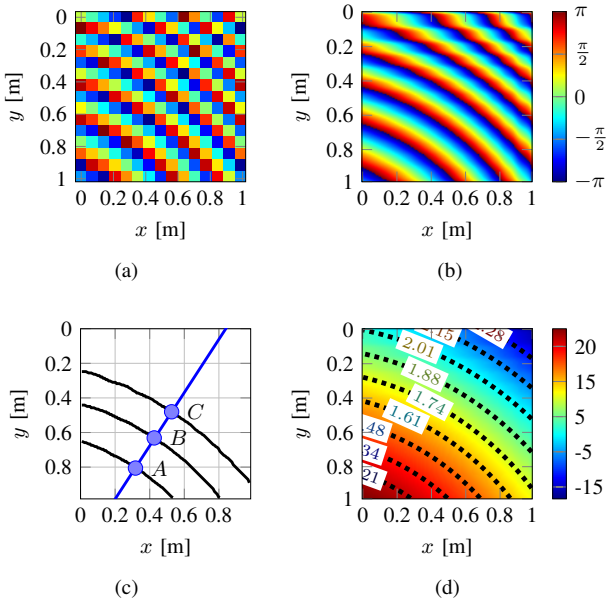

Fig. 5. The process steps of the proposed method. (a) The phase distribution of the directly sampled E-field, (b) the phase distribution of the interpolated E-field, (c) the intersection of phase fronts and the line crossed the beam axis, and (d) the phase distribution of the unwrapped E-field and the radius fronts. The numbers on the dotted line show the values of radii.

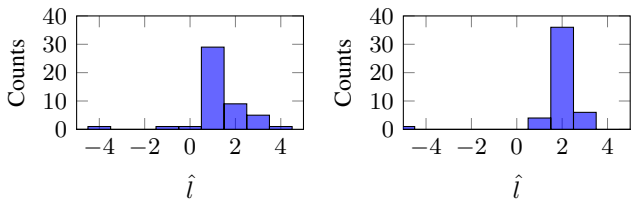

Fig. 6. The histograms of the estimation results using the proposed method. (a) $l = 1$, (b) $l = 2$.

Let $\Delta\rho_1 = \overline{AB}$ and $\Delta\rho_2 = \overline{BC}$, and we can determine the position of the beam axis using (7). Finally, according to the obtained beam axis and the phase gradient method, we can estimate the OAM mode via unwapped E-field shown in Fig. 5(d). The results are shown in Fig. 6. For the transmitting OAM mode $l = 1$ and $l = 2$, the bin counts of values 1 and 2 reach the maximum. The results show that the proposed method can accurately estimate the corresponding OAM mode.

IV. Conclusion

In this article, an OAM mode estimation method with unknown beam axis is proposed. The main idea of the proposed method is to first estimate the position of the beam axis and then use the phase gradient method to estimate the OAM mode. The simulation results proved the effectiveness of the method. Future work will focus on conducting experiments and analyzing the errors of each step in detail.

REFERENCES

[1] V. Ivaška and V. Kalesinskas, "Vortical electromagnetic waves with a stationary power flow," in *18-th International Conference on Microwaves, Radar and Wireless Communications*, pp. 1–4, Jun. 2010.

[2] L. Allen, M. W. Beijersbergen, R. J. C. Spreeuw, and J. P. Woerdman, "Orbital angular momentum of light and the transformation of Laguerre-Gaussian laser modes," *Physical Review A*, vol. 45, pp. 8185–8189, Jun. 1992.

[3] B. Thidé, H. Then, J. Sjöholm, K. Palmer, J. Bergman, T. D. Carozzi, Y. N. Istomin, N. H. Ibragimov, and R. Khamitova, "Utilization of Photon Orbital Angular Momentum in the Low-Frequency Radio Domain," *Physical Review Letters*, vol. 99, p. 087701, Aug. 2007.

[4] M. Veysi, C. Guclu, F. Capolino, and Y. Rahmat-Samii, "Revisiting Orbital Angular Momentum Beams: Fundamentals, Reflectarray Generation, and Novel Antenna Applications," *IEEE Antennas and Propagation Magazine*, vol. 60, no. 2, pp. 68–81, 2018.

[5] G. Shu, W. Wang, D. Liang, Y. Deng, R. Wang, H. Zhang, and N. Li, "Chirp Signal Transmission and Reception With Orbital Angular Momentum Multiplexing," *IEEE Antennas and Wireless Propagation Letters*, vol. 18, pp. 986–990, May 2019.

[6] K. Zhang, Y. Wang, Y. Yuan, and S. N. Burokur, "A Review of Orbital Angular Momentum Vortex Beams Generation: From Traditional Methods to Metasurfaces," *Applied Sciences*, vol. 10, pp. 1141–1153, Feb. 2020.

[7] A. G. White, C. P. Smith, N. R. Heckenberg, H. Rubinsztein-Dunlop, R. McDuff, C. O. Weiss, and C. Tamm, "Interferometric Measurements of Phase Singularities in the Output of a Visible Laser," *Journal of Modern Optics*, vol. 38, no. 12, pp. 2531–2541, 1991.

[8] J. F. Nye, M. V. Berry, and F. C. Frank, "Dislocations in wave trains," *Proceedings of the Royal Society of London. A. Mathematical and Physical Sciences*, vol. 336, no. 1605, pp. 165–190, 1974.

[9] M. J. Padgett, F. M. Miatto, M. P. J. Lavery, A. Zeilinger, and R. W. Boyd, "Divergence of an orbital-angular-momentum-carrying beam upon propagation," *New Journal of Physics*, vol. 17, p. 023011, Feb. 2015.

[10] S. M. Mohammadi, L. K. S. Daldorff, K. Forozesh, B. Thidé, J. E. S. Bergman, B. Isham, R. Karlsson, and T. D. Carozzi, "Orbital angular momentum in radio: Measurement methods," *Radio Science*, vol. 45, no. 4, 2010.

[11] E. Cano and B. Allen, "Multiple-antenna phase-gradient detection for OAM radio communications," *Electronics Letters*, vol. 51, no. 9, pp. 724–725, 2015.

[12] T. D. Drysdale, B. Allen, E. Cano, Q. Bai, and A. Tennant, "Evaluation of OAM-radio mode detection using the phase gradient method," in *2017 11th European Conference on Antennas and Propagation (EUCAP)*, pp. 3606–3610, 2017.

[13] M. Xie, X. Gao, M. Zhao, W. Zhai, W. Xu, J. Qian, M. Lei, and S. Huang, "Mode Measurement of a Dual-Mode Radio Frequency Orbital Angular Momentum Beam by Circular Phase Gradient Method," *IEEE Antennas and Wireless Propagation Letters*, vol. 16, pp. 1143–1146, 2017.

[14] Y. Hu, S. Zheng, Z. Zhang, H. Chi, X. Jin, and X. Zhang, "Simulation of orbital angular momentum radio communication systems based on partial aperture sampling receiving scheme," *IET Microwaves, Antennas & Propagation*, vol. 10, no. 10, pp. 1043–1047, 2016.

[15] T. D. Drysdale, B. Allen, and C. Stevens, "Discretely-sampled partial aperture receiver for orbital angular momentum modes," in *2017 IEEE International Symposium on Antennas and Propagation USNC/URSI National Radio Science Meeting*, pp. 1431–1432, 2017.

[16] Q. Feng, J. Liang, and L. Li, "Variable Scale Aperture Sampling Reception Method for Multiple Orbital Angular Momentum Modes Vortex Wave," *IEEE Access*, vol. 7, pp. 158847–158857, 2019.

[17] S. Yu, L. Li, and N. Kou, "Generation, reception and separation of mixed-state orbital angular momentum vortex beams using metasurfaces," *Optical Materials Express*, vol. 7, pp. 3312–3321, Sep. 2017.

[18] M. L. N. Chen, L. J. Jiang, and W. E. I. Sha, "Detection of Orbital Angular Momentum With Metasurface at Microwave Band," *IEEE Antennas and Wireless Propagation Letters*, vol. 17, no. 1, pp. 110–113, 2018.

[19] M. L. Chen, L. J. Jiang, and W. E. Sha, "Orbital Angular Momentum Generation and Detection by Geometric-Phase Based Metasurfaces," *Applied Sciences*, vol. 8, p. 362, Mar. 2018.

[20] A. Voors, "NEC based antenna modeler and optimizer." https://www.qsl.net/4nec2/, Accessed 12/06/2021.